Lecture Notes in Mechanical Engineering

Y. V. D. Rao · C. Amarnath ·
Srinivasa Prakash Regalla ·
Arshad Javed ·
Kundan Kumar Singh *Editors*

Advances in Industrial Machines and Mechanisms

Select Proceedings of IPROMM 2020

Springer

Lecture Notes in Mechanical Engineering

Lecture Notes in Mechanical Engineering (LNME) publishes the latest developments in Mechanical Engineering—quickly, informally and with high quality. Original research reported in proceedings and post-proceedings represents the core of LNME. Volumes published in LNME embrace all aspects, subfields and new challenges of mechanical engineering. Topics in the series include:

- Engineering Design
- Machinery and Machine Elements
- Mechanical Structures and Stress Analysis
- Automotive Engineering
- Engine Technology
- Aerospace Technology and Astronautics
- Nanotechnology and Microengineering
- Control, Robotics, Mechatronics
- MEMS
- Theoretical and Applied Mechanics
- Dynamical Systems, Control
- Fluid Mechanics
- Engineering Thermodynamics, Heat and Mass Transfer
- Manufacturing
- Precision Engineering, Instrumentation, Measurement
- Materials Engineering
- Tribology and Surface Technology

To submit a proposal or request further information, please contact the Springer Editor of your location:

China: Ms. Ella Zhang at ella.zhang@springer.com
India: Priya Vyas at priya.vyas@springer.com
Rest of Asia, Australia, New Zealand: Swati Meherishi
at swati.meherishi@springer.com
All other countries: Dr. Leontina Di Cecco at Leontina.dicecco@springer.com

To submit a proposal for a monograph, please check our Springer Tracts in Mechanical Engineering at http://www.springer.com/series/11693 or contact Leontina.dicecco@springer.com

Indexed by SCOPUS. All books published in the series are submitted for consideration in Web of Science.

More information about this series at http://www.springer.com/series/11236

Y. V. D. Rao · C. Amarnath ·
Srinivasa Prakash Regalla · Arshad Javed ·
Kundan Kumar Singh
Editors

Advances in Industrial Machines and Mechanisms

Select Proceedings of IPROMM 2020

Springer

Editors
Y. V. D. Rao
Department of Mechanical Engineering
Birla Institute of Technology and Science
Pilani-Hyderabad Campus
Hyderabad, Telangana, India

Srinivasa Prakash Regalla
Department of Mechanical Engineering
Birla Institute of Technology and Science
Pilani-Hyderabad Campus
Hyderabad, Telangana, India

Kundan Kumar Singh
Department of Mechanical Engineering
Birla Institute of Technology and Science
Pilani-Hyderabad Campus
Hyderabad, Telangana, India

C. Amarnath
Department of Mechanical Engineering
Indian Institute of Technology Bombay
Mumbai, Maharashtra, India

Arshad Javed
Department of Mechanical Engineering
Birla Institute of Technology and Science
Pilani-Hyderabad Campus
Hyderabad, Telangana, India

ISSN 2195-4356 ISSN 2195-4364 (electronic)
Lecture Notes in Mechanical Engineering
ISBN 978-981-16-1768-3 ISBN 978-981-16-1769-0 (eBook)
https://doi.org/10.1007/978-981-16-1769-0

This Springer imprint is published by the registered company Springer Nature Singapore Pte Ltd.
The registered company address is: 152 Beach Road, #21-01/04 Gateway East, Singapore 189721, Singapore

Contents

Space Applications and Modern Structures

Bio-medical Devices and Bio-mechanisms, Devices for Aerospace, Automobile and Railways

About the Editors

Prof. Y. V. D. Rao is currently an Associate Professor at the Department of Mechanical Engineering, Birla Institute of Technology and Science (BITS), Pilani, Hyderabad campus. He obtained his B.Tech. (Mechanical Engineering) from National Institute of Technology, Surathkal (Known that time as Regional Engineering College); M.Tech. (Design Eng.) from the Indian Institute of Technology, Delhi (IITD); and Ph.D. from the Government College of Engineering, Raipur (Known now as NIT Raipur). His major areas of research interest include topological synthesis and analysis of Gear trains and Robotic structures, Robot-Assisted Incremental Sheet Metal Forming, Vibration and Shock Isolation, Robotic Dental Implantation, and Crashworthiness in automobile vehicles under axial impacts. He has published 18 papers in peer-reviewed international journals. He has so far published 40 plus research works in national and international conferences.

Prof. C. Amarnath is a Mechanical Engineering Graduate of 1968. After earning his Ph.D in the area of Mechanism Synthesis and Design, he joined IIT Bombay as a faculty member and has held several senior positions like Head of Dept. and Dean at IITB. He was heading SINE, the Innovation, Entrepreneurship, and Incubation Centre, at IIT Bombay till his retirement from service in 2012. Prof. Amarnath has several publications to his credit and has established the Robotics Lab, the Textile Lab, and the Innovation Centre at IITB. He is a consultant to several industries like L&T, Godrej, BHEL, and Nuclear Power Corporation. Major projects undertaken by him (some as member of a team) include a Spiral Heat Exchanger Mfg. Machine (L&T), Push-Pull Mechanism for NPC, Six legged walking machine (BRNS-BARC), and a Remotely Operated Robot for the Army Technology Board. Prof. Amarnath was instrumental in establishing and is the current President of the Association for Machines and Mechanisms. He was recently bestowed the Distinguished Service award by IFToMM, the International Federation.

Prof. Srinivasa Prakash Regalla is currently a Professor at the Department of Mechanical Engineering, Birla Institute of Technology and Science, Pilani, Hyderabad campus. He obtained his B.Tech. (Mech.) from Kakatiya University, Warangal; M.Tech. (Mech.) from the Indian Institute of Technology, Kanpur; and Ph.D. from the

Indian Institute of Technology, Delhi. His major areas of research interests include computer-aided mechanical design, additive manufacturing, tribology in sheet metal forming, biomechanics, and design of medical devices. He has published 50 papers in respected international journals and two books on product design. Dr. Regalla received the BIRAC-BIG grant award in 2014 for prosthetic design and distinguished alumni award from his B.Tech. college.

Dr. Arshad Javed is currently an Assistant Professor at the Department of Mechanical Engineering, Birla Institute of Technology and Science, Pilani (BITS Pilani), Hyderabad Campus. He obtained his B.Tech. (Mechanical Engg.) from BIET Jhansi(UP) and M.E. (Mechanical Engg.) and Ph.D. from BITS Pilani, Pilani Campus. His teaching and research interests include Topology Optimization, Robotics, Mechatronics, Automation, and Microfluidic systems. He has published 15 papers in respected international journals and presented several research works in National and International conferences.

Dr. Kundan Kumar Singh is currently an Assistant Professor at the Department of Mechanical Engineering, Birla Institute of Technology and Science, Pilani (BITS Pilani), Hyderabad Campus. He obtained his B.Tech. (Mechanical Engg.) from JGEC Jalpaiguri (WB); MME (Mechanical Engg.) from Jadavpur University, Kolkata (WB); and Ph.D. from Indian Institute of Technology Bombay, Mumbai, India. His teaching and research interests include machine tool dynamics, manufacturing automation, micro manufacturing, surface metrology, data analysis, and condition monitoring. He has published 9 papers in reputed international journals and presented several research works in National and International conferences.

Compliant Mechanism

Jacobian-Based Inverse Kinematics Analysis of a Pneumatic Actuated Continuum Manipulator

Mrunal Kanti Mishra, Sambaran Ghosal, Arun Kumar Samantaray, and Goutam Chakraborty

1 Introduction

Continuum manipulators are biologically inspired manipulators. These draw inspiration from a variety of biological species such as snakes [1], octopus arms [2], or elephant trunks [3]. They have gathered huge research interests in the past decades owing to the inherent flexibility of their designs. These manipulators are day by day finding new application areas especially in the fields where rigid link manipulators are not feasible, i.e., in workspaces with a large number of barriers or obstacles. The development of closed-form models for these kinds of manipulators is a challenge.

Over the past decades, numerous planar and spatial kinematics models are developed for continuum manipulators. Some of these include the Cosserat Rod model [4], Elastic Beam theory [5], or even a lumped model [6]. For instance, as a planar forward kinematics model, a serpentine curve is designed which closely matches the kinematics of a snake's body in two dimensions as it crawls across the ground [1]. On the other hand, Chirikjian [4] fitted a mathematical curve to a high degree of freedom hyper-redundant manipulator. However, due to computational complexity, a few continuum robots match the proposed curve. Jones and Walker [5] used an Elastic Beam theory to develop an FK model and validated it on a multi-section continuum manipulator. Giri and Walker [6] discretized a continuum arm to a three-module lumped element model and studied FK. Escande et al. [7] studied the FK of a multi-section bionic manipulator with the help of the triangulation method. They

M. K. Mishra (✉) · S. Ghosal · A. K. Samantaray · G. Chakraborty
Indian Institute of Technology Kharagpur, Kharagpur 721302, West Bengal, India
e-mail: mrunalkanti@gmail.com

A. K. Samantaray
e-mail: samantaray@mech.iitkgp.ac.in

G. Chakraborty
e-mail: goutam@mech.iitkgp.ac.in

Y. V. D. Rao et al. (eds.), *Advances in Industrial Machines and Mechanisms*,
Lecture Notes in Mechanical Engineering,
https://doi.org/10.1007/978-981-16-1769-0_1

have validated the developed method by coupling the continuum manipulator along with six degrees of freedom conventional rigid manipulator. Mishra et al. [8] developed a closed-form solution for a single segment continuum manipulator using an elliptical integral approach. The model approximates an Euler–Bernoulli beam as a continuum manipulator in planar space. A geometrical approach-based FK is also developed which relates between actuator zone-based parameters and the pose of the manipulator, which assumes the section to be a constant cross-section. As a result, the deflected manipulator takes a circular shape with a constant radius of curvature, and so the model is named as constant curvature model [9]. This model is proved a remarkable approach across a wide variety of continuum manipulator designs due to its analytical attractiveness.

Continuum manipulators are those having infinite degrees of freedom, involving more flexibility and reachability of targets. This redundancy can be exploited for the avoidance of obstacles, elimination of singularities, and as well as for smooth motion tasks realizing. Inverse kinematics modelling of continuum manipulators remains difficult to obtain because they are under-determined systems with a high number of unknown parameters. Moreover, most of the governing IK equations are highly nonlinear in nature, which does not even have closed-form solutions. The inability to solve these high nonlinear equations leads most of the researchers towards numerical methods or model-free methods. Neppalli et al. [10] developed the IK for a continuum manipulator using the geometrical approach. They tried to find the solutions by inverting the continuum curvature model for a single section only. However, this method fails to determine the solutions for multi-section manipulator. Chirikjian [11] proposed an IK model using a backbone curve. The same authors also developed a modal approach to calculate actuator zone parameters [12]. This method gives a very accurate result, but because of its complicacy, it is very difficult to use. Braganza et al. [13] used a feed-forward neural network to control nine degrees of freedom OctArm -V. Similarly, Li et al. [14] used a model-free method based on the Kalman filter to control a continuum manipulator.

Most of the aforementioned IK models either fail to describe the pose in closed form or computationally complex to solve. This in turn implies an inability to develop an effective model-based controller in real time. Therefore, in this paper, we use the constant curvature model to arrive at the FK equations. After the FK model, we develop the IK solutions for the manipulator by using the pseudo-Jacobian method. The developed method is validated on Robotino-XT (see Fig. 1), which consists of a two-segment continuum manipulator named as CBHA.

The outline of the paper is organized as follows. A brief introduction on the kinematics of different kinds of continuum robots is provided in Sect. 1. In Sect. 2, the forward kinematics using Continuum Curvature Model along with the proposed Jacobian-based inverse kinematics model is presented. The proposed model is applied on a serially connected two-stage bionic continuum manipulator and the results for the same are given in Sect. 3. Finally, in Sect. 4, some concluding comments are specified.

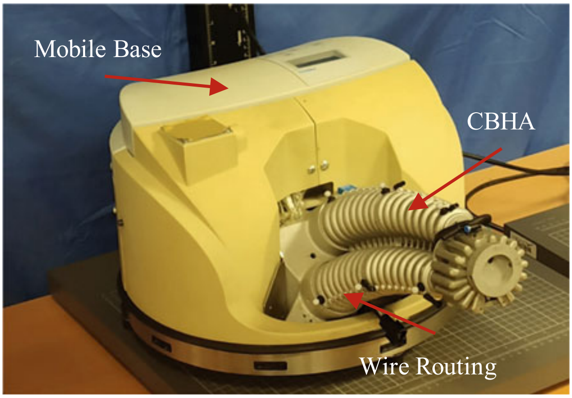

Fig. 1 Robotino-XT: CBHA with a mobile base

2 Kinematic Modelling

2.1 Forward Kinematics

Forward Kinematics of bending sections of continuum manipulators is widely developed under the constant curvature assumption [9]. This model is particularly based on two different assumptions. Firstly, the entire manipulator is separated into multiple numbers of segments. This approximation allows converting the infinite degrees of freedom system to a finite one. Secondly, the shape of a bending section is to be a perfect arc of a circle or the curvature radius is constant throughout the length. This approximation has the advantage to simplify the model formulations for some continuum manipulators and allow easy formulations of matrix transformation.

Continuum Curvature model is obtained by using two independent mappings as shown in Fig. 2. The explicit mapping is varied from manipulator to manipulator and mostly depends on the number of actuators per segment. This mapping maps actuator zone parameters (length of the actuators) to configuration zone parameters (segment arc parameters). On the other hand, the typical mapping is applied to all types of

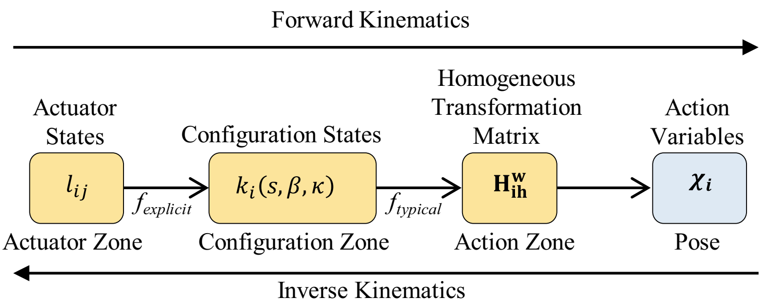

Fig. 2 Systematic model procedure for forward and inverse kinematics

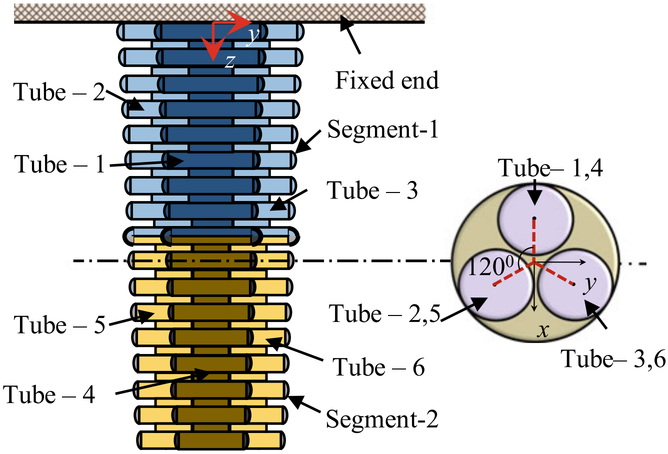

Fig. 3 Two-segment manipulator with cross-section

continuum manipulators, regardless of lengths and orientation. This mapping maps configuration zone parameters to action zone parameters, i.e., manipulator pose.

A continuum manipulator segment can be actuated by j—number of actuators. However, for several reasons, three actuators per segment with 120° actuator spacing type continuum manipulator is best suitable to move a manipulator spatially [9]. These kinds of manipulators are energy efficient and have great manoeuverability than other choices of actuator numbers and actuator spacing. So, in this paper, a two-segment continuum manipulator along with three actuators per segment having 120° actuator spacing is considered. The manipulator along with its cross-sectional area is shown in Fig. 3. The mapping between the actuator lengths $\left(l_{ij}\right)$ and the segment arc parameters ($\boldsymbol{k}_i(s_i, \beta_i, \kappa_i)$) for three actuators per segment with 120° actuator spacing is determined as [5]

$$\begin{aligned} s_i\left(l_{ij}\right) &= \tfrac{l_{i1}+l_{i2}+l_{i3}}{3} \\ \beta_i\left(l_{ij}\right) &= \operatorname{atan2}\left(\sqrt{3}(l_{i3}-l_{i2}), l_{i2}+l_{i3}-2l_{i1}\right) \\ \kappa_i\left(l_{ij}\right) &= \tfrac{2\sqrt{l_{i1}^2+l_{i2}^2+l_{i3}^2-l_{i1}l_{i2}-l_{i2}l_{i3}-l_{i3}l_{i1}}}{(l_{i1}+l_{i2}+l_{i3})r_{s_i}} \end{aligned} \tag{1}$$

and the mapping between the arc parameters and the manipulator pose of a segment is determined by a transformation matrix as [9]

$$\mathbf{H}_{i\mathbf{h}}^{i\mathbf{b}} = \begin{bmatrix} \cos\kappa_i s_i \cos\beta_i & -\sin\beta_i & \sin\kappa_i s_i \cos\beta_i & \frac{\cos\beta_i(1-\cos\kappa_i s_i)}{\kappa_i} \\ \cos\kappa_i s_i \sin\beta_i & \cos\beta_i & \sin\kappa_i s_i \sin\beta_i & \frac{\sin\beta_i(1-\cos\kappa_i s_i)}{\kappa_i} \\ -\sin\kappa_i s_i & 0 & \cos\kappa_i s_i & \frac{\sin\kappa_i s_i}{\kappa_i} \\ 0 & 0 & 0 & 1 \end{bmatrix} \tag{2}$$

where s is the segment length, β is the segment angle, κ is the segment radius of curvature, l is the length of the actuator for i th segment and j th actuator, r_s is the radius of each segment, and $\mathbf{H}_{i\mathbf{h}}^{i\mathbf{b}}$ is the homogeneous matrix for ith segment. Note that, under the same actuation to the actuators of a section, the lengths of the actuators are the same, resulting in the orientation of the segment to a null matrix and the head frame position of the segment to $\begin{bmatrix} 0 \ 0 \ s_i \end{bmatrix}^{\mathbf{T}}$.

Using the relations from (1) and (2), the tip rotation matrix and position vector of a two-segment continuum manipulator with respect to the world frame is given as

$$\mathbf{H}_{2\mathbf{h}}^{\mathbf{w}} = \mathbf{H}_{1\mathbf{b}}^{\mathbf{w}} \prod_{\varsigma=1}^{2} \left(\mathbf{H}_{\varsigma\mathbf{h}}^{\varsigma\mathbf{b}} \mathbf{H}_{(\varsigma+1)\mathbf{b}}^{\varsigma\mathbf{h}} \right), \ \mathbb{R} \in [4 \times 4] \tag{3}$$

where $\prod(\cdot)$ calculates product summation of the transformation matrices. Note that, in the end section of the manipulator, $\mathbf{H}_{(\varsigma+1)\mathbf{b}}^{\varsigma\mathbf{h}}$ is an $[4 \times 4]$ identity matrix. From (3), the pose of the tip of a segment in the Cartesian frame is portrayed by

$$\boldsymbol{\chi} = \begin{bmatrix} \theta_x \ \theta_y \ \theta_z \ x \ y \ z \end{bmatrix}^{\mathrm{T}} \tag{4}$$

where $\theta_x = \text{atan2}\big(-\mathbf{H}_{2\mathbf{h}}^{\mathbf{w}}(2,3), \mathbf{H}_{2\mathbf{h}}^{\mathbf{w}}(2,3)\big)$, $\theta_y = \text{atan22}\big(-\mathbf{H}_{2\mathbf{h}}^{\mathbf{w}}(1,3), \mathbf{H}_{2\mathbf{h}}^{\mathbf{w}}(3,3)\big)$, $\theta_z = 0$, $x = \mathbf{H}_{2\mathbf{h}}^{\mathbf{w}}(1,4)$, $y = \mathbf{H}_{2\mathbf{h}}^{\mathbf{w}}(2,4)$, $z = \mathbf{H}_{2\mathbf{h}}^{\mathbf{w}}(3,4)$. Note that p, q of $\mathbf{H}(p,q)$ are matrix row and column, respectively. The rotation of the manipulator along the central axis (θ_z) is equal to zero, because the manipulator is only allowed to a two-way bending, and no torsional moment is allowed. Therefore, we will omit θ_z from our further derivation and consider the pose of the manipulator tip to be five degrees of freedom.

2.2 Differential Kinematics

Differential kinematics of a continuum manipulator can be determined by applying the first derivative with respect to time to forward kinematics relation. Therefore, applying first time derivative to (4) results,

$$\dot{\boldsymbol{\chi}} = \mathbf{J}(l)\dot{\boldsymbol{l}}(t), \ \mathbb{R} \in [5 \times 1] \tag{5}$$

where $\mathbf{J}(\boldsymbol{l})$ is the Jacobian matrix and can be determined by applying chain rule as

$$\mathbf{J}(\boldsymbol{l}) = \frac{\partial \boldsymbol{\chi}}{\partial \boldsymbol{l}} = \frac{\partial \boldsymbol{\chi}}{\partial \mathbf{H}} \frac{\partial \mathbf{H}}{\partial \boldsymbol{k}} \frac{\partial \boldsymbol{k}}{\partial \boldsymbol{l}}, \ \mathbb{R} \in [5 \times 3n]. \tag{6}$$

From (6), it can be checked that $\frac{\partial \boldsymbol{\chi}}{\partial \mathbf{H}} \in \mathbb{R}^{(5\times16)}$ is independent of a number of segments of the manipulator. However, for instance, for a two-segment manipulator, $\frac{\partial \mathbf{H}}{\partial \boldsymbol{k}} \in \mathbb{R}^{(16\times6)}$ and $\frac{\partial \boldsymbol{k}}{\partial \boldsymbol{l}} \in \mathbb{R}^{(6\times6)}$ depend on the number of segments of the manipulator.

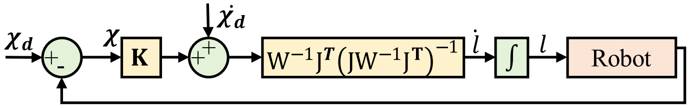

Fig. 4 Block diagram for inverse kinematics using Jacobian

2.3 Inverse Kinematics

In order to move the manipulator pose in a certain trajectory, it is essential to find actuator zone parameters from the action zone parameters. Thus, it is crucial to develop inverse kinematics solutions correctly. To develop a model-based controller for a class of continuum manipulator, in this paper, a Jacobian matrix is developed using the differential kinematics equation as of (6). However, no direct procedure is available to invert the rectangular Jacobian matrix. So, a weighted matrix is used for pseudo-Jacobian inverse $\left(\mathbf{J}^{\dagger}\right)$, where $\mathbf{J}^{\dagger} = \mathbf{J}^{\mathbf{T}}\left(\mathbf{J}\mathbf{J}^{\mathbf{T}}\right)^{-1}$. So, using resolved rate algorithm, a weighting matrix [15], and a gain matrix, the actuator state velocities $\dot{\boldsymbol{l}}(t)$ can be determined as

$$\dot{\boldsymbol{l}}(t) = \mathbf{W}^{-1}\mathbf{J}^{\mathrm{T}}\left(\mathbf{J}\mathbf{W}^{-1}\mathbf{J}^{\mathrm{T}}\right)^{-1}\left(\dot{\boldsymbol{\chi}}_{d} + \mathbf{K}\left(\boldsymbol{\chi}_{d} - \boldsymbol{\chi}\right)\right) \tag{7}$$

where the weighting matrix is a diagonal matrix and is defined as

$$\mathbf{W} = diag\left(w_1\ w_2\ \ldots\ w_n\right),\ \mathbb{R} \in [3n \times 3n] \tag{8}$$

where the weight values are chosen in such a way to avoid joint limits. In addition, the gain matrix is defined by

$$\mathbf{K} = diag\left(\hbar_1\ \hbar_2\ \ldots\ \hbar_5\right),\ \mathbb{R} \in [5 \times 5] \tag{9}$$

where the gain values are chosen as positive values. This matrix is usually a diagonal matrix, which reduces the tracking errors between actual $\boldsymbol{\chi}$ and desired $\boldsymbol{\chi}_d$. Additionally, integration of the actuator zone velocities $\dot{l}_{ij}(t)$ is performed to find actuator zone parameters/trajectory $l_{ij}(t)$. The block diagram for IK is given in Fig. 4.

3 Results and Discussion

The developed kinematics formulations can be verified on a n–segment continuum manipulator. However, for simplicity, the effectiveness of the developed model is validated on Robotino-XT, which contains a CBHA attached to a mobile base with 48° angle as shown in Fig. 1. The mobile base of Robotino-XT can move and rotate individually on a horizontal surface and the CBHA is a two-stage pneumatic actuated continuum manipulator. Each manipulator segment consists of three flexible tubes with 120° spacing and each tube is attached with a flexible string. The strings help to measure the length of the tubes at any stage. The flexible tubes are actuated by an external compressor with a maximum allowable pressure of 2 bar. The differential pressures of the tubes of each segment ultimately help the manipulator to bend about a certain axis. The tubes are made of flexible material, namely polyamide. The geometric parameters of the manipulator are provided in Table 1.

The workspace of the Robotino-XT depends on the individual actuation of the mobile base and CBHA. The mobile base can move horizontally to any position in any direction, whereas the CBHA can move spatially depending upon the actuation pressure. Therefore, the workspace of the Robotino-XT is assumed as a *rectanguloid* of a certain height. In this paper, only pneumatic actuation is supplied to the CBHA and the actuation of the mobile base is given zero. The lengths of each tube of the actuated CBHA is measured by the attached strings and by using the Continuum Curvature model, the workspace of the manipulator is determined in local coordinate as shown in Fig. 5 [8].

The desired trajectory is required to validate the derived formulations from the workspace of the continuum manipulator. Therefore, within the workspace of the CBHA, the reference trajectory for a circle is chosen as

Table 1 Geometric parameters of a two-segment continuum manipulator

Symbol	Unit	Range
Tube length (actuator length)	(mm)	90–125
Tube volume	(10^5 mm^3)	1.52–2.046
Average segment diameter	(mm)	107.8

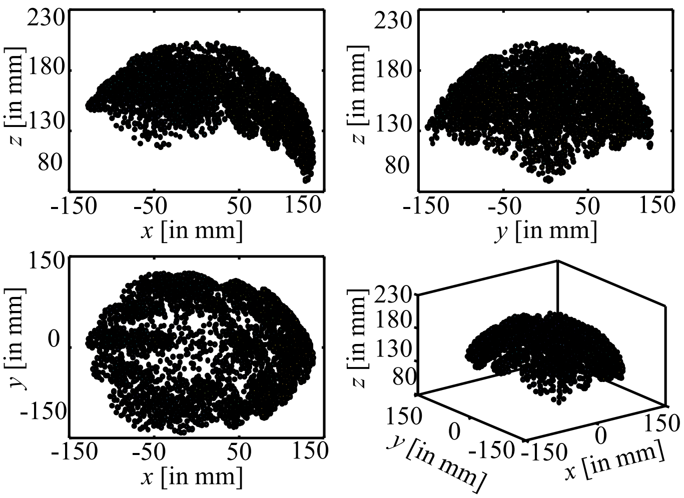

Fig. 5 Workspace of CBHA

$$\begin{aligned} x(t) &= 90\cos 0.52t\,(\text{mm}) \\ y(t) &= -5 + 90\sin 0.52t\,(\text{mm}) \\ z(t) &= 180(\text{mm}) \end{aligned} \tag{10}$$

where $x(t)$, $y(t)$, $z(t)$ are the required trajectory for the pose of the manipulator end effector. The tip orientation is omitted from the current analysis. The accuracy of the actual trajectory mentioned in (10) is verified by comparing the output of the inverse kinematics solution (obtained using (7)) by inseting it into the forward kinematics model and observing the differences in the trajectories. In Fig. 6, the weight matrix values are kept constant for all manipulator trajectories, whereas the gain values are varied suitably to improve the accuracy. It is found that an increase in the gain values increases the accuracy significantly. A detailed inspection shows that only by changing the third and the fourth gain values, the accuracy changes. This is because we have considered $x(t)$, $y(t)$ as variables and $z(t)$ as constant. Moreover, any changes in the first and second gain values do not affect the trajectory, because the tip orientations have no specific significance for the trajectory pose.

We defined the period to complete the desired circle to be 12 s and set the weighting matrix $\mathbf{W} = \text{diag}(1, 1, 1, 0.5, 1, 1)$, and gain matrix $\mathbf{K} = \text{diag}(0.005, 0.005, 10, 10, 0.05)$. During this time, the manipulator end-effector pose is varied sinusoidally as shown in Fig. 7. From the figure, it is seen that the x, y tip coordinates approximately achieved the desired trajectory. However, a significant error occured in z coordinate as the trajectory tracking progresses. This can be further improved by improving the gain values.

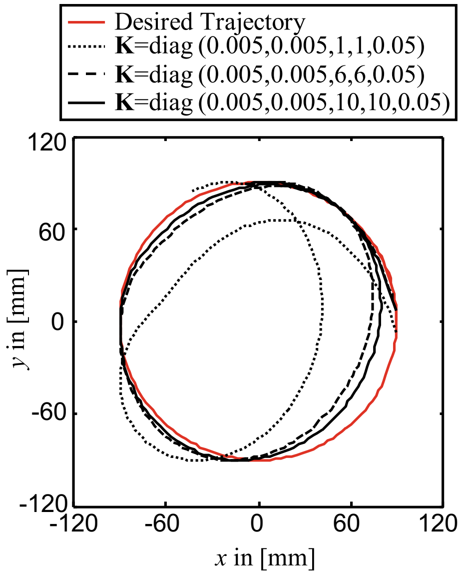

Fig. 6 A circular Desired trajectory versus Actual trajectory

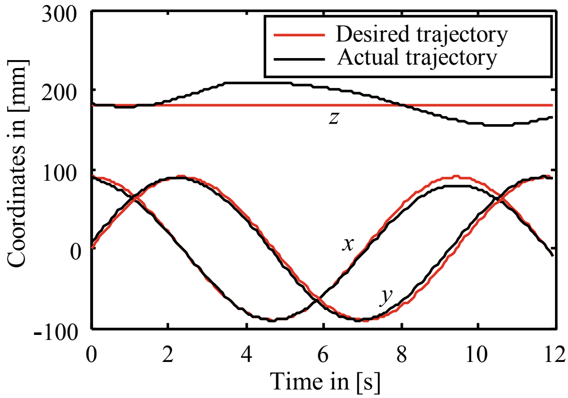

Fig. 7 Manipulator tip position over the period of time

The average positional error of the manipulator tip for optimized weight and gain values is compared with previously developed inverse kinematics methods as shown in Table 2. Previously developed methods are based on model-free techniques whereas the current method is based on model-based techniques. For the desired trajectory, the lengths of all the six actuators are determined from the proposed model in Fig. 4. The length variation of the actuators is displayed in Fig. 8.

Table 2 Error comparison of different methods

Authors	Manipulator	Method	Error (mm)
Braganza et al. [13]	OctArm-V	Feed-forward neural network	30
Li et al. [14]	Pneumatic actuator muscle	Adaptive Kalman filter	2.31
Present method	Two-stage Elephant trunk like manipulator	Resolved rate algorithm	3.51

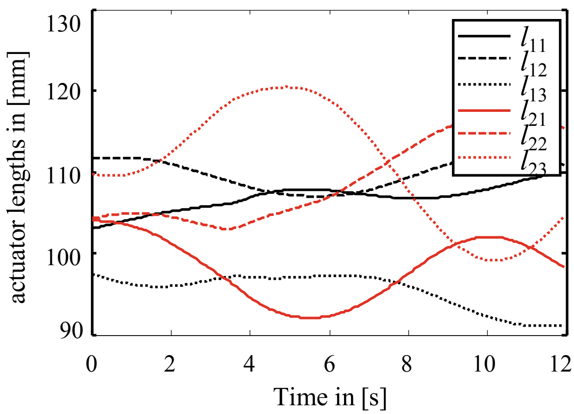

Fig. 8 Actuator length variation according to differential kinematics

4 Conclusion

In this paper, a closed-form inverse kinematics model is developed using the pseudo-Jacobian inverse method and applied on CBHA of Robotino-XT, which is a two-segment continuum manipulator. A circular trajectory is chosen from the workspace of the manipulator to validate the proposed model. The method discussed above assumes a suitable weighting matrix and a gain matrix. The weighting matrix helps in weight distribution to the actuators, so that inverse of the diagonal Jacobian matrix can be performed. However, changing the values does not help to increase accuracy. The gain matrix tracks the error in the desired and current pose of the manipulator and helps to increase the tip positional accuracy. It is observed that, with an increase in certain gain values, the manipulator pose accuracy increases. In future, the proposed model-based method can help to develop an effective real-time controller to manoeuvre the manipulator smoothly.

References

1. Hirose, S.: Biological Inspired Robots, Snake-Like Locomotors and Manipulators. Oxford University Press, Oxford (1993)
2. Kang, R., Branson, D.T., Guglielmino, E., Caldwell, D.G.: Dynamic modeling and control of an octopus inspired multiple continuum arm robot. Comput. Math Appl. **64**(5), 1004–1016 (2012)
3. Mishra, M.K., Samantaray, A.K., Chakraborty, G., Jain, A., Pathak, P.M., Merzouki, R.: Dynamic modelling of an elephant trunk like flexible bionic manipulator. In: International Mechanical Engineering Congress & Exposition 2019, vol. 4, pp. 1–9. ASME, Salt Lake City (2019). https://doi.org/10.1115/IMECE2019-11113
4. Chirikjian, G.S.: Hyper-redundant manipulator dynamics: a continuum approximation. Adv. Robot. **9**(3), 37–41 (1995)
5. Jones, B.A., Walker, I.D.: Kinematics for multisection continuum robots. IEEE Trans. Robot. **22**(1), 43–55 (2006)
6. Giri, N., Walker, I.D.: Three module lumped element model of a continuum arm section. In: IEEE/RSJ International Conference on Intelligent Robots and Systems 2011, pp. 4060–4065. IEEE, San Franscisco (2011)
7. Escande, C., Chettibi, T., Merzouki, R., Coelen, V., Pathak, P.M.: Kinematic calibration of a multisection bionic manipulator. IEEE/ASME Trans. Mechatron. **20**(2), 663–674 (2015)
8. Mishra, M.K., Samantaray, A.K., Chakraborty, G., Pachouri, V., Pathak, P.M., Merzouki, R.: Kinematics model of bionic manipulator by using elliptic integral approach. In: 4th International and 19th National Conference on Machines and Mechanisms. Springer, Mandi (2019)
9. Webster III, R.J., Jones, B.A.: Design and kinematic modeling of constant curvature continuum robots: a review. Int. J. Robot. Res. **29**(13), 1661–1683 (2010)
10. Neppalli, S., Csencsits, M.A., Jones, B.A., Walker, I.D.: Closed-Form inverse kinematics for continuum manipulators. Adv. Robot. **23**, 2077–2091 (2009)
11. Chirikjian, G.S.: A general numerical method for hyper-redundant manipulator inverse kinematics. In: IEEE International Conference on Robotics & Automation 1993, pp. 107–112. IEEE, Atlanta (1993)
12. Chirikjian, G.S., Burdick, J.W.: A modal approach to hyper-redundant manipulator kinematics. IEEE Trans. Robot. Autom. **10**(3), 346–354 (1994)

13. Braganza, D., Dawson, M.D., Walker, I.D., Nath, N.: A neural network controller for continuum robots. IEEE Trans. Rob. **23**(5), 1270–1277 (2007)
14. Li, M., Kang, R., Branson III, D.T., Dai, J.S.: Model-free control for continuum robots based on an adaptive kalman filter. IEEE/ASME Trans. Mechatron. **23**(1), 286–297 (2018)
15. Chan, T.F., Dubey, R.V.: A weighted least-norm solution based scheme for avoiding joint limits for redundant joint manipulators. IEEE Trans. Robot. Autom. **11**(2), 286–292 (1995)

Path Curvature Theory: A Classic and Effective Design Tool

Mattia Cera, Marco Cirelli, Ettore Pennestrì, Pier Paolo Valentini, and V. R. Shanmukhasundaram

1 Introduction

The planar path curvature analysis is a well-known classic topic in kinematics. Two centuries of scientific investigations created a formidable cultural heritage, as well as a great source of knowledge and inspiration for mechanical engineers. This paper has the purpose to discuss applications of this theory to three industrial cases: the stability of lifting rigs, the design of centrifugal dampers, and the analysis of compliant linkages. These topics seem more related to dynamics and elasticity than to curvature kinematics.

The first part is dedicated to the modeling of a body resting on two curves [1]. When the curves are circles, this model reproduces the dynamics of a four-bar coupler subjected to the weight force. A geometric criterion for the stability analysis of lifting rigs will be established. The second part is dedicated to the computation of tautochrone oscillation period T of a particle moving along an epicycloid and subjected to a centrifugal force field. The derivation of an analytical expression of T is based on a novel application of the fundamental formulas of Cesàro's intrinsic geometry. The obtained result is meaningful for the tuning of centrifugal dampers [2, 3]. The last application regards an application of Euler–Savary equation to compliant linkages.

M. Cera · E. Pennestrì (✉) · P. P. Valentini
University of Rome Tor Vergata, 00133 Rome, Italy
e-mail: pennestri@mec.uniroma2.it
URL: https://www.uniroma2.it:

M. Cirelli
Niccolò Cusano University, 00166 Rome, Italy
e-mail: marco.cirelli@unicusano.it

V. R. Shanmukhasundaram
Birla Institute of Technology and Science, Department of Mechanical Engineering, Pilāni, India

Y. V. D. Rao et al. (eds.), *Advances in Industrial Machines and Mechanisms*,
Lecture Notes in Mechanical Engineering,
https://doi.org/10.1007/978-981-16-1769-0_2

2 Oscillations of a Body Resting on Two Curves

As depicted in Fig. 1, a body with two points A and B is sliding without friction along the curves $\mathcal{C}_A$ and $\mathcal{C}_B$, respectively. The body is initially in equilibrium under the gravity force. Our purpose is to obtain the period T of small oscillations. In this section, it will be demonstrated how such period is related to the system geometric parameters. It will be also discussed how the theory of planar curvature offers a concise solution to the final result.

The following nomenclature is adopted:

- A_1, B_1 positions of points A and B after a body rotation;
- g acceleration of gravity;
- G and G_1 initial and final positions of the center of mass, respectively;
- k_G radius of gyration;
- L_{eq} length of equivalent simple pendulum;
- M and N orthogonal projections of P and P_0 along directions $\Omega_B P_0$ and $\Omega_A P - 0$, respectively;
- m mass of the moving cylinder;
- I_G body moment of inertia about center of mass G;
- P_0 and P initial and final positions of the velocity pole, respectively;
- x, y coordinates of P in a Cartesian system of coordinates with origin in P_0 and axes along horizontal and vertical directions;
- ϕ infinitesimal rotation angle of bar AB;
- Ω_A, Ω_B centers of curvature of trajectories of A and B, respectively;

Fig. 1 Oscillations of a body resting on two curves

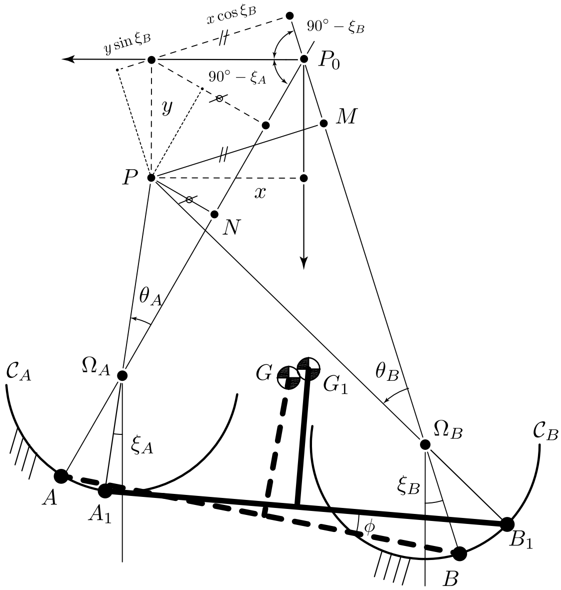

– θ_A, θ_B infinitesimal angles of rotations of segments $\Omega_A A$ and $\Omega_B B$, respectively;
– ξ_A, ξ_B angles formed by segments $\Omega_A A$ and $\Omega_B B$ with vertical direction, respectively.

From the system geometry, the following equalities can be deduced:

$$\widehat{AA_1} = \Omega_A A \cdot \theta_A = P_0 A \cdot \phi \tag{1a}$$

$$\widehat{BB_1} = \Omega_B B \cdot \theta_B = P_0 B \cdot \phi \tag{1b}$$

$$\widehat{G_0 G} = P_0 G_0 \cdot \phi \tag{1c}$$

Moreover, the lengths of infinitesimal arcs $\widehat{MP}$ and $\widehat{NP}$ are

$$\widehat{MP} = \Omega_B P \cdot \theta_B \, , \quad \widehat{NP} = \Omega_A P \cdot \theta_A \tag{2}$$

For the equilibrium, the distance x is required. This distance will be computed solving the system

$$\begin{cases} x \cos \xi_B + y \sin \xi_B = \Omega_B P \cdot \theta_B \\ x \cos \xi_A - y \sin \xi_A = \Omega_A P \cdot \theta_A \end{cases} \tag{3}$$

or

$$x = \frac{\Omega_B P \cdot \theta_B \sin \xi_A + \Omega_A P \cdot \theta_A \sin \xi_B}{\sin (\xi_A + \xi_B)} \tag{4}$$

The Aronhold-Kennedy theorem yields

$$\theta_B = \frac{P_0 B}{\Omega_B B} \phi \, , \quad \theta_A = \frac{P_0 A}{\Omega_A A} \phi \tag{5}$$

The substitution of (5) into (4) gives

$$x = \frac{\dfrac{\Omega_B P_0 \cdot P_0 B}{\Omega_B B} \sin \xi_A + \dfrac{\Omega_A P_0 \cdot P_0 A}{\Omega_A A} \sin \xi_B}{\sin (\xi_A + \xi_B)} \phi \tag{6}$$

Taking the moments about P, we have the governing differential equations of motion

$$\left(k_G^2 + P_0 G^2\right) \frac{\mathrm{d}^2 \phi}{\mathrm{d}t^2} + g \left(G_0 G + x\right) \phi = 0 \tag{7}$$

Since $G_0 G = P_0 G \phi$, the length of an equivalent pendulum can be expressed as

Fig. 2 Equivalent symmetric four-bar linkage

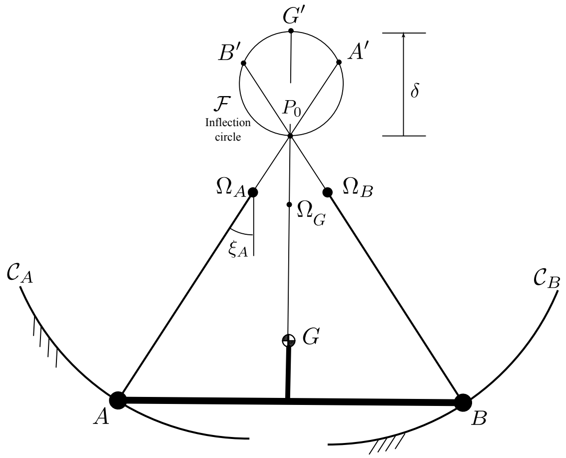

$$\frac{k_G^2 + P_0G^2}{L_{eq}} = P_0G + \frac{\Omega_B P_0 \cdot P_0 B}{\Omega_B B} \frac{\sin \xi_A}{\sin(\xi_A + \xi_B)} + \frac{\Omega_A P_0 \cdot P_0 A}{\Omega_A A} \frac{\sin \xi_B}{\sin(\xi_A + \xi_B)} \tag{8}$$

To gain insights, it is useful to particularize the previous equation for the case of a point mass ($k_G = 0$) on the coupler of a symmetric four-bar linkage (see Fig. 2) such that $\xi_A = \xi_B$, $\Omega_A A = \Omega_B B$, $P_0 A = P_0 B$.

Under these conditions, Eq. (8) simplifies into

$$\frac{P_0G^2}{L_{eq}} = P_0G + 2\frac{\Omega_B P_0 \cdot P_0 B}{\Omega_B B} \frac{\sin \xi_A}{\sin 2\xi_A} \tag{9}$$

One can verify that[1]

$$G'P_0 = P_0B \frac{\Omega_B P_0}{\Omega_B B \cos \xi_A} \tag{10}$$

Therefore, from Eq. (9), we can conclude that

$$L_{eq} = \frac{P_0G^2}{P_0G + G'P_0} = \frac{P_0G^2}{G'G} = \Omega_G G \tag{11}$$

The result confirms that in some cases, the theory of curvature offers a concise solution for preliminary stability and natural frequency analysis of one degree of freedom mechanical systems. An application is the test of the stability of suspension

[1] Considered that $P_0G' \cos \xi_A = P_0B'$, the proportion (10) gives

$$(\Omega_B P_0 - \Omega_B B) : \Omega_B B = \left(P_0B' - P_0B\right) : P_0B$$

This leads to the second form of the Euler–Savary equation $P_0B^2 = \Omega_B B \cdot B'B$ specialized for point B.

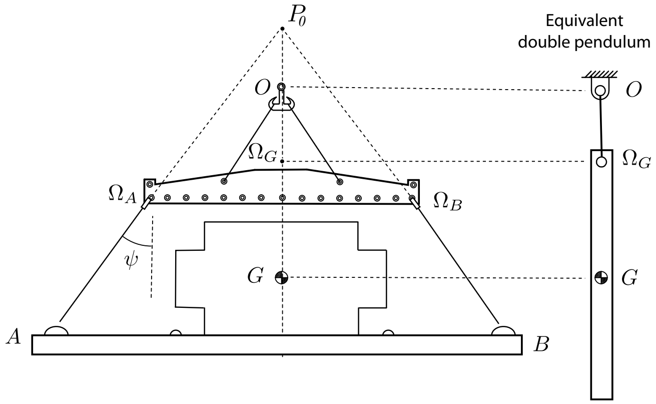

Fig. 3 Stability of lifting rigs

rigs [4, 5]. With reference to Fig. 3, the stability for small oscillations about the equilibrium position of the suspended load requires the position of center of curvature Ω_G to lie between suspension point O and center of mass G:

$$\therefore \qquad P_0O < P_0\Omega_G < P_0G \tag{12}$$

In particular, the beam mass is assumed negligible and the system motion can be considered as that of a double pendulum suspended at O, with $O\Omega_G$ the first massless bar and $\Omega_G G$ the second bar. In terms of readily measured segment lengths, after Euler–Savary equation:

$$\frac{1}{P_0O} > \frac{1}{P_0G} + \left(\frac{1}{P_0A} - \frac{1}{P_0\Omega_A}\right)\cos\psi \tag{13}$$

3 Curvature Theory and Design of Centrifugal Dampers

Centrifugal dampers are key components of modern internal combustion engines with a reduced number of cylinders and increased energy output at lower engine speeds [2]. In Ref. [6], a kinematic equivalence between a four-bar linkage and the new generation of centrifugal dampers has been established. The main components are counterweights where their centers of mass are constrained to move along given tautochrone[2] trajectories (e.g., cycloids or epicycloids) [3, 7]. In this section, we will

[2]Given a field of forces F, a curve $\mathcal{C}$ is said to be *tautochrone* with respect to a point O if a particle starting from rest, moving along $\mathcal{C}$ under the action of F, arrives at point O after an interval of time T which is independent from the point starting position.